J Am Oil Chem Soc (2009) 86:1163–1173
DOI 10.1007/s11746-009-1464-6

ORIGINAL PAPER

Physical Properties of Rice Bran Wax in Bulk and Organogels

Lakmali Samuditha K. Dassanayake · Dharma R. Kodali · S. Ueno · K. Sato

Received: 16 April 2009 / Revised: 15 July 2009 / Accepted: 22 July 2009 / Published online: 1 September 2009

Abstract Differential scanning calorimetry (DSC), optical microscopy, and X-ray diffraction (XRD) were used to examine the thermal behavior, crystal structure, and crystal morphology of rice bran wax (RBX) in bulk and oil–wax mixtures, and to compare them with those of carnauba wax (CRX) and candellila wax (CLX). The RBX employed in the present study was separated from rice bran oil by winterization, filtration, refinement, bleaching, and deodorization. The RBX crystals melted in the bulk state at 77–79 °C with $\Delta H_{\text{melting}} = 190.5$ J/g, which is quite large compared with CLX (129 J/g) and CRX (137.6 J/g). XRD data of the RBX crystals revealed $O_{\perp}$ subcell packing and a long spacing value of 6.9 nm. Thin long needle-shaped crystals were observed in the mixtures of RBX and liquid oils [olive oil and salad oil (canola:soy bean oil = 50:50)]; therefore, the dispersion of RBX crystals in these liquid oils was much finer than that of CRX and CLX crystals. Organogels formed when the mixture of every plant wax and liquid oil was melted at elevated temperature and cooled to ambient temperature. However, the mixture of RBX and olive oil at a concentration ratio of 1:99 wt.% formed an organogel at 20 °C, whereas the lowest concentration necessary for CRX to form an organogel in olive oil was 4 wt.% and that for CLX was 2 wt.%. Observation of the rate of gel formation using DSC and viscosity measurements indicated that the gel structure formed soon after RBX crystallized, whereas a time delay was observed between the organogel formation and wax crystallization of CRX and CLX. These results demonstrate RBX's good organogel-forming properties, mostly because of its fine dispersion of long needle like crystals in liquid oil phases.

Keywords Organogels · Rice bran wax · Crystal morphology · X-ray diffraction · Viscosity · Hardness · Thermal stability

L. S. K. Dassanayake · S. Ueno · K. Sato (✉)
Laboratory of Food Biophysics,
Graduate School of Biosphere Science,
Hiroshima University, Kagamiyama 1-4-4,
Hiroshima 739-8528, Japan
e-mail: kyosato@hiroshima-u.ac.jp

L. S. K. Dassanayake
e-mail: lakmali@hotmail.com

D. R. Kodali (✉)
Global Agritech Inc., 710, Olive Ln,
Minneapolis, MN 55447, USA
e-mail: kodali@globalagritech.us

D. R. Kodali
Department of Bioproducts and Biosystems Engineering,
University of Minnesota, 1390 Eckles Avenue,
St Paul, MN 55108, USA

Introduction

Organogels have attracted attention as promising oil-structuring systems for *trans*-fat alternative hardstocks [1–8]. Organogels are viscoelastic materials comprised of organic gelators and liquid oils [3]. In these semi-solid systems, the liquid oil phase is immobilized by a three-dimensional network of self-assembled, inter-twined gelator fibers [9]. Quite recently, different types of organogels have been employed in cosmetics, deodorants, and hair-care materials [4]. Such organogels are also significant food materials because they have enhanced softness, easy handling, quick melting, spreadability, easy film formation, and water-barrier properties, as observed in the organogels used in phytosterols and sterol esters [10, 11], fatty acids and fatty alcohols [12–14], 12-hydroxy-stearic acid

[15–18], ricinoelaidic acid [19, 20], sorbitan monostearate [21] and ceramides [22].

In addition to these organogelating materials, waxes may also be highly promising. Wax is a fatty substance that contains long hydrocarbon chains with or without a functional group [23–26]. Functional groups that are often present in waxes include alcohol, ester, ketone, and aldehyde. The wax esters derived from plants, insects and marine animals are used in various industrial applications (e.g. cosmetics, lubricants, polishes, surface coatings, inks, and foods) [24, 27]. Current consumer demands are moving toward the use of bio-based waxes rather than mineral-based waxes for utilization in the food, cosmetic, and pharmaceutical industries. One group of bio-based waxes available on a massive scale is the plant wax group, which represents the esters of long-chain fatty acids and long-chain aliphatic alcohols. However, research on organogels using plant waxes is rather limited. Toro-Vazquez et al. [5] and Morales-Rueda et al. [28] recently reported on the physical properties of organogels using candellila wax (CLX) and dotriacontane in safflower oil. The present research mainly sought to understand the physical properties of organogels prepared by RBX. The gel formation, gelation kinetics, thermal behavior, crystallization, morphological features at microscopic level, and hardness of the wax–oil organogels were analyzed.

Rice (*Oryza sativa*) bran wax is a natural plant wax derived from rice bran, which is a byproduct of rice milling. It is a major wax resource in East Asia, where rice is the main food [29]. The content of wax in rice bran oil varies with extraction conditions. Wax in crude rice bran oil is removed by a dewaxing step in the refining process. The refining of rice bran oil usually includes dewaxing, degumming, deacidification, bleaching, deodorization, and winterization [25–27]. The potential applications of RBX in the cosmetic, pharmaceutical, food, polymer, and leather industries are as cost-efficient as those of other plant waxes, such as carnauba wax (CRX) and CLX [26]. With relatively high melting points of 78–81 °C, RBX easily crystallizes at ambient temperatures, resulting in a finely dispersed mixture with liquid oil [30]. The present study demonstrates that with different types of liquid oil, RBX crystals easily form organogels.

Experimental

Materials and Sample Preparation

RBX, CRX, and CLX were supplied by Global Agritech, Inc., Minneapolis, MN USA. Table 1a lists the specifications of RBX and Table 1b presents the chemical compositions of three waxes. The approximate chemical composition of CRX (wt.%) is aliphatic and aromatic esters, 84–85% (containing aliphatic esters 40%, ω-hydroxy esters 13%, cinnamic aliphatic diesters 8%); free fatty acids 3–3.5%; alcohols 2–3%; lactides 2–3%; hydrocarbons 1–3%; resins 4–6%; moisture and inorganic residues 0.5–1% [31]. The composition of CLX is 49–50% *n*-alkanes, 20–29% esters of acids and alcohols with even-numbered carbon chains (C28–34), 12–14% alcohols and sterols; and 7–9% free acids [28]. As a reference, we employed tripalmitoyl-glycerol (PPP), which was purchased from Sigma Chemicals, Japan (purity, 99%).

Table 1 Chemical properties of rice bran wax (RBX)

(a) Specifications of RBX

Property	Typical analysis	Range
Melting point (°C)	78	77–79
Acid value (mg KOH/g)	6.3	3–8
Iodine value	11.4	8–15
Saponification value (mg KOH/g)	86.3	80–90

(b) Chemical composition

Carbon number	Fatty acid (wt.%)			Fatty alcohol (wt.%)		
	RBX[a]	CLX[b,c]	CRX[c]	RBX[a]	CLX[b,c]	CRX[b,c]
16	3.6	2		–	–	
18	2.3	1	*	–	–	
20	5.3	12	*	–	–	
22	26.1	4	*	–	5	
24	40.5	1	*	3.5	–	
26	11.5	1	*	8.4	3	
28	6.6	7	*	14.0	9	7
30	3.1	32		26.4	65	16
32	1.0	33		19.6	15	60
34	–	7		16.5	3	17
36	–			9.2		
38	–			2.4		

[a] Present study

[b] Ref. [32]

[c] Ref. [33] (*means only the presence, not the amount)

To form organogels, RBX, CLX, and CRX were blended with salad oil (canola:soybean oil = 50:50) [C16:0 8.3%, C18:1 38.1%, C18:2 40.3%, C18:3 7.9%] (Nisshin OilliO, Japan), olive oil (J-Oil Mills, Japan), and liquid paraffin (Wako Chemicals, Japan) at 0.2–4.0 wt.% levels. Samples were prepared by dissolving the weighed solid waxes in a weighed amount of liquid oil at 80 °C, which was sufficient to obtain full melting of all components. The heated solutions were subsequently cooled to room temperature (20 °C) and stored at this temperature. All concentrations discussed here are expressed as a weight percentage (wt.%).

Thermal Analysis and Phase Diagram Construction

To construct the phase diagram of RBX in liquid oil, the melting points of RBX crystals in liquid paraffin, salad oil, and olive oil were measured in mixtures with different RBX concentrations of 1, 2, 3, 4, 5, 10, 15, 20, 25, 30, 40, 50, and 100 wt.%. The heated solutions were subsequently cooled to room temperature (20 °C) and stored at this temperature.

The melting temperature (T_m) and crystallization temperature (T_c) of three waxes in pure bulk states and in RBX–salad oil organogel states were also determined. The T_m and T_c of waxes and wax–liquid oil mixtures were determined by differential scanning calorimetry (DSC) using a Rigaku DSC-8240 calorimeter (Rigaku, Tokyo, Japan). Samples (10–15 mg) were hermetically sealed in aluminum pans, heated from room temperature to 100 °C, then cooled to 0 °C and heated again to 100 °C. The rate of temperature variation was 2 °C/min for heating and cooling. Peak T_m, T_c, melting enthalpy (ΔH_m), and crystallization (ΔH_c) were determined using the software provided with the instrument. DSC measurements were carried out in triplicate for every RBX concentration in liquid oils. The average endothermic peak value was taken as the T_m of each wax concentration. The average melting point values were plotted against the wax concentration to obtain the phase diagram of RBX–oil mixtures.

Crystallization and Gel Formation

The crystallization of RBX was carefully observed in two experiments. In the first experiment, three plant waxes (RBX, CRX, and CLX) were crystallized in olive oil. The waxes and olive oil mixtures were prepared by adding appropriate amounts of solid waxes to 15 g of olive oil in 2.5-cm-diameter test tubes. Each oil–wax mixture was heated to 80 °C in a water bath while shaking to dissolve the waxes in the liquid oil. The resulting homogeneous solutions were cooled to 20 °C and subjected to visual observation until the appearance of crystals was confirmed under quiescent conditions.

In the second experiment, the effects of liquid oils on the crystallization of RBX were observed by using salad oil, olive oil, and liquid paraffin. In addition, the formation of organogels was observed by using the three liquid oils with RBX concentrations of 0.2, 0.5, 1.0, 2.0, and 4.0 wt.% in the solutions. The mixtures were heated to 80 °C for complete melting of the waxes, then cooled and kept at 20 °C to observe gelation. The gelation time was measured as the duration until the oil stopped flowing due to hand shaking.

Crystal Morphology

The wax crystals formed in olive oil, liquid paraffin, and salad oil were observed with polarized optical microscopy. The crystal morphologies of RBX, CRX, and CLX were compared at the same solute concentration of 1 wt.%. The mixtures of the three waxes and liquid oils were prepared by adding an appropriate amount of waxes to the liquid oils and heating to 80 °C to form a homogenous solution. The solutions were cooled to room temperature without stirring until wax crystals formed. The crystals were observed by polarized light microscopy using an Olympus CX31 PF optical microscope (Olympus Optical Co., Ltd., Japan). A small amount of sample containing crystals was placed on a glass microscope slide and gently covered with a glass cover slip. Digital images of partially and fully polarized specimens were acquired using an Olympus DP12-2 camera (Olympus Corporation, Japan).

Viscosity Measurements

The viscosity of the plant wax–vegetable oil organogels was measured during cooling using a Vibro Viscometer SV-10 (A & D, Japan) with a Thermo-mate BF 400 (Yamato, Japan). This viscometer uses a frequency of 30 Hz at a constant frequency and amplitude. The cooling and heating rates were not constant and depended on the viscometer itself. The effect of the type of plant wax on the viscosity of the organogels was measured for 1% (w/w) of RBX and CLX in olive oil.

The prepared gel samples were heated to 80 °C for complete melting. The melted sample was placed in the sample cell of the viscometer at 80 °C, and two gold-plated paddle sensors were immersed in the sample. The viscosity change of the sample was then measured with respect to the temperature during cooling from 80 to 20 °C. The measured viscosity values for each sample were plotted against the temperature, and these viscosity profiles were analyzed by comparison with the DSC thermographs.

Hardness Measurements

An EX–120–E Penetrometer (Elex Scientific, Tokyo, Japan) was used to measure the hardness of the organogels made of RBX, CRX, and CLX in olive oil. The sample cups in which the samples were kept during the measurement had an internal diameter of 5.5 cm and a depth of 3.4 cm. This sample cup included a glass container filled with water to maintain constant temperature during the measurement. The internal diameter of the glass container was 10.7 cm, and its depth was 6 cm. The conical plastic probe of the penetrometer had a base diameter of

16.25 ± 0.015 mm, a cone height of 7.075 ± 0.015 mm, and a weight of 9.38 ± 0.025 g. A load weighing 50 g was placed on the sample in each penetration. The penetration depth was measured three times for each sample at 20 °C, and average values were calculated.

X-ray Diffraction Analysis

X-ray diffraction (XRD) studies of bulk RBX, CLX and CRX and wax–olive oil mixtures were made by using an RINT-2000 X-Ray Diffractometer (Rigaku, Tokyo, Japan). Sample holders with sample wells (0.5 mm depth) were loaded with samples at room temperature. Angular scans (2θ) were performed from 1.2 to 27 °C using a Cu source ($\lambda = 0.154$ nm) X-ray tube at 30 kV and 250 mA. Small-angle X-ray scattering (SAXS) and wide-angle X-ray scattering (WAXS) measurements were performed at 20 °C.

Results and Discussion

The specifications of RBX are presented in Table 1a. The melting point of RBX is 78 ± 1 °C. The acid value is 6.3 mg KOH/g, the iodine value is 11.4, and the saponification value is 86.3 mg KOH/g.

Most of the wax esters in their natural form contain small amounts of sterols, sterol esters, fatty alcohols, fatty acids, and resinous matter. The plant wax esters after refining mainly contain esters of fatty acids and fatty alcohols of different chain lengths. The chemical composition of fatty acid and fatty alcohol moieties of RBX presented in Table 1b. The RBX measured in this study contains esters of fatty acids varying from 16 to 32, and fatty alcohols of carbon numbers varying from 24 to 38. Taking into account the high concentrations of carbon numbers of 22 and 24 for the fatty acid moiety, and 30 and 32 for the fatty alcohol moiety, we assume that the most abundant wax esters contain total carbon numbers of 52, 54, and 56. The high-temperature GC analysis reported by Vali et al. [26] corroborates this observation with the molecular species having carbon numbers 52, 54 and 56 being the major peaks in the chromatogram. This property may be a unique feature of RBX having long-chain fatty acids and fatty alcohol esters. CLX contains hydrocarbons (*n*-alkanes) of 50–55% with $C_{31,}$ the principal component—hentriacontane [28, 32]. In addition, it contains esters of fatty acids with carbon numbers varying from 16 to 34, and fatty alcohols with carbon numbers varying from 22 to 34 with free fatty acids and free fatty alcohols (Table 1b). The large range of chain lengths gives rise to the large range in the esters [32]. However, Tulloch [32] reported that, CRX contains 36% monoesters and 11% free alcohols of 47% total volatiles. Tada et al. [33] reported that the presence of fatty acids, carbon numbers varying from 18 to 28, and fatty alcohols of carbon numbers varying from 28 to 34 with the abundance of C_{32} fatty alcohols. As noted by Letcher [31] and others [34] CRX contains mainly fatty esters (80–85%), free alcohols (10–15%), acids (3–6%) and hydrocarbons (1–3%). As a peculiarity, carnauba wax contains esterified fatty dialcohols (diols, about 20%), hydroxylated fatty acids (about 6%) and cinnamic acid (about 10%). As materials derived from natural sources, these waxes with different compositions exhibit various physical behaviors which are unique to each material.

Figure 1 depicts DSC cooling and heating thermopeaks of RBX, CLX, and CRX in pure bulk states examined during cooling to 0 °C after melting at 100 °C, and reheating (0–100 °C) from the first-crystallized materials. Irrespective of the gelator concentration and the cooling and heating rates employed in this study, the three waxes showed broader DSC melting peaks with indefinite start and blunt maximum indicating the presence of a series of different solid substances. However, RBX exhibits single melting and crystallization profiles, while CLX and CRX exhibit multiple melting and crystallization profiles. The molecular compositional differences explain the thermal behavior of these waxes. RBX, containing a single chemical class of wax esters of aliphatic fatty acids esterified to fatty alcohols, gives more uniform single melting and crystallization peaks. However, CRX and CLX contain multiple chemical classes and hence exhibit complex melting and crystallization behavior.

To characterize the melting and crystallization behavior of CLX and CRX revealing such multiple DSC patterns, we took the values of melting temperature (T_m) and crystallization temperature (T_c) at the peaks of highest-temperature endothermic patterns during the heating process

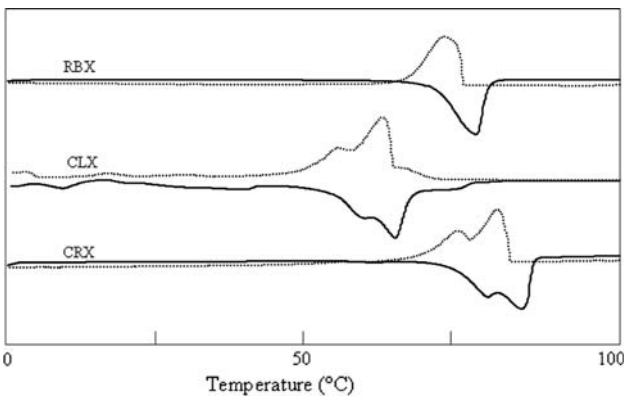

Fig. 1 DSC patterns taken during cooling (*dotted line*) and heating (*solid line*) processes of rice bran wax (*RBX*), carnauba wax (*CRX*) and candellila wax (*CLX*) in bulk states

and exothermic patterns during the cooling process. The values of melting enthalpy (ΔH_m) and melting entropy (ΔS_m) were obtained for a single endothermic peak for RBX, and for the summation of major endothermic peaks. Table 2 summarizes T_m, ΔH_m, and ΔS_m of RBX, CLX, and CRX. The thermal stability expressed as T_m increases in the order of CLX < RBX < CRX. However, the values of ΔH_m and ΔS_m do not follow the ordering of the T_m values: the value of ΔH_m of RBX is larger than that of CRX by 40% and larger than that of CLX by 50%. The same tendency was observed for ΔS_m values. Quite interestingly, ΔH_m and ΔS_m of RBX are very close to those of PPP, rather than those of CRX and CLX. The ΔH_m and ΔS_m values indicate cohesive energy for the packing of molecules in the crystal structure.

Toro-Vazquez et al. [5] described that the presence of different *n*-alkanes (nonacosane, tritriacontane etc.) in CLX might develop a mixed molecular packing with hentriacontane during cooling which caused multiple melting and crystallization profiles. Therefore we can assume that the long chain fatty acid and fatty alcohol esters present in RBX do not tend to form such mixed self-assembled structures with a lower extent of three-dimensional molecular structure (i.e. lower crystallinity and ΔH_m). In addition, RBX exhibited comparatively high self assembly capability and this is confirmed by the longer crystal dimension with birefringence of the structures as shown below.

Figure 2 presents optical micrographs of the crystals of RBX in olive oil, liquid paraffin, and salad oil, and CRX and CLX (1% w/w) in olive oil taken at room temperature. In the first micrograph, we compare the crystal morphology of RBX with CLX and CRX in olive oil prepared by moderate cooling without stirring. Although details of the organogel-forming properties will be described later, it must be mentioned here that at the 1% w/w level of wax in olive oil, only RBX was in a gel state, whereas CLX and CRX were in a viscous sol state. Accordingly, the crystal morphologies of the three waxes in olive oil were quite different. The morphology of RBX crystals was very long (20–50 μm) needles, which is a desirable feature for gel formation [1]. The crystal morphology of CRX and CLX differs from RBX, with spherulitic structures having a diameter of less than 10 μm that are not conducive to the formation of organogels. Whereas the long needle like structures of RBX form good crystal matrices that mesh well at the intercrystalline interfaces to form organogels. This enables one to entrap large volumes of liquid oils in the crystalline scaffolding. Similar observations were reported by Morales-Rueda et al. [28] for CLX and pure *n*-alkanes, i.e. dotriacontane (C_{32}). Regarding the effects of liquid oils on the crystal morphology of RBX, no difference was observed in crystal morphology between olive oil and salad oil; however, the RBX crystals in liquid paraffin were rather round and are not conducive to the formation of organogels. Several researchers reported the strong influences of the gelator composition on crystal size, shape and rheology of organogels developed in edible oils [11–13, 28]. The presence of different molecular components in the wax seemed to have profound effect on the crystal habit of the plant wax–vegetable oil organogels. Also the conditions of organogel preparation (e.g. stirring or rate of cooling), and storage conditions can affect the crystal morphology of the gelators [5, 10]. Therefore, the influence of rapid cooling with mechanical disturbance on the crystal morphology and gel formation of plant wax–vegetable oil organogels needs to be evaluated.

Table 2 Thermal properties of plant waxes (rice bran wax, RBX, CLX, CRX and tripalmitoyl-glycerol (*PPP*)

	T_m (°C)	ΔH_m (J/g)	ΔS_m (mJ/g/K)
RBX	76	190.5	559.0
CLX	64	129.0	376.1
CRX	84	137.6	384.6
PPP	66.4	209.6	609.3

Figure 3 displays the XRD patterns of RBX crystals in bulk and wax–oil mixtures (olive oil, RBX concentration of 1% w/w). The wide-angle diffraction peaks of 0.415 and 0.373 nm indicating orthorhombic perpendicular ($O_\perp$) subcell packing are observed in the bulk state and wax–oil mixtures. In this connection, it may be valuable to refer to the fact that the crystals of triacylglycerols are packed in three different polymorphs (α, β', and β) with hexagonal, $O_\perp$, and triclinic parallel ($T_{//}$) subcell packings [23, 24]. Among the three polymorphs, the fat crystals of β' polymorph exhibit better properties for functionality like smooth texture and better mouth-feel in margarine and shortening because of its crystal morphology, dispersability and optimal melting property [24, 35]. The wide-angle XRD patterns of the three wax crystals having peaks of 0.41 and 0.37 nm are similar to those of the β' form of triacylglycerols. However, only RBX revealed much clear and prominent small-angle diffraction peaks compared to CRX and CLX both in bulk state and wax–oil mixtures. The long spacings were calculated from the (003) reflections of the small-angle diffraction patterns as 6.9 nm. The XRD patterns of RBX–olive oil mixture exhibited the same small-angle and wide-angle peaks as those in the bulk state, although a broad peak due to liquid oil appeared in the wide-angle region.

The results on the intensity of XRD diffraction peaks shown in Fig. 3 may be related to the morphology of the RBX crystals. The intensity of the long spacing patterns was remarkably weaker than that of the short spacing

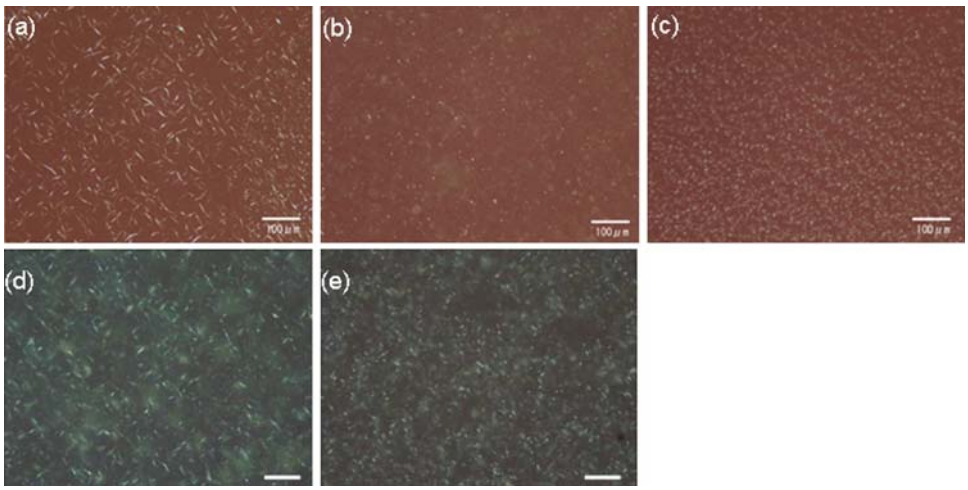

Fig. 2 Optical micrographs of wax crystals in liquid oils (1% w/w): (**a**) RBX in olive oil, (**b**) CLX in olive oil, (**c**) CRX in olive oil (**d**) RBX in liquid paraffin and (**e**) RBX in salad oil taken at 20 °C. Scale bar, 100 μm

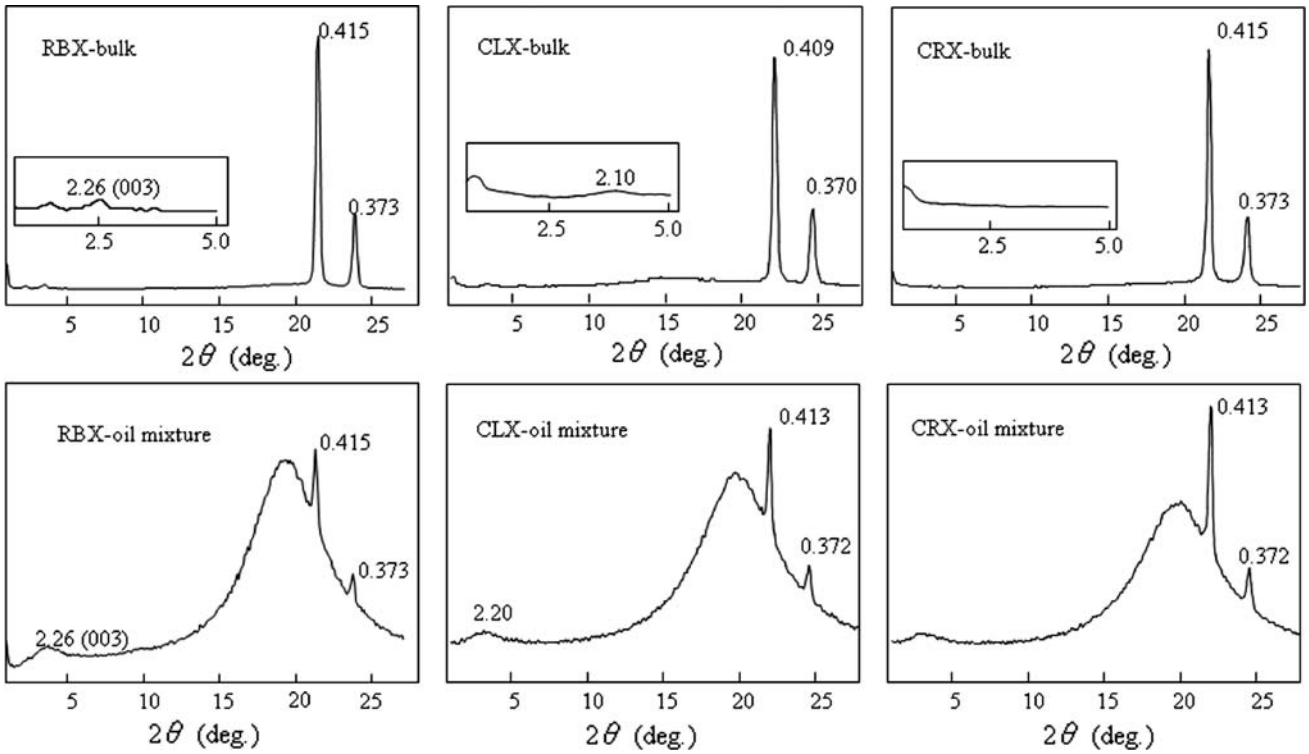

Fig. 3 X-ray diffraction wide-angle and small-angle patterns of RBX, CLX and CRX crystals in bulk state and 8% w/w wax–oil mixtures (olive oil) taken at 20 °C. The small-angle pattern of the bulk data is enlarged in the *boxes*

patterns. In general, such a contrast in the XRD diffraction peak intensity between the long and short spacing patterns is related to strong anisotropy in crystal growth rates between the directions vertical to the lamellar plane and within the lamellar plane. If the growth rate vertical to the lamellar plane is slower than that within the lamellar plane, quite thin crystals having needle or platelet morphology are formed, showing very weak long spacing patterns and stronger short spacing patterns. In the case of RBX crystals, the long linear molecular structure having on average 54 carbons together with polar interactions at the ester-bond region may provide strong attractive interactions within the lamellar plane and weak interactions among the lamellar plane through $-CH_3$ end groups. This property may explain the difference in the XRD peaks of the long and short spacing patterns of the RBX crystals.

Figure 4 plots the T_c and T_m of RBX in salad oil–RBX mixtures at different RBX concentrations. The peak temperatures of DSC cooling and heating thermopeaks were chosen as the T_c and T_m of RBX throughout the entire range of RBX concentrations in the RBX–salad oil mixtures. As the melting point of salad oil (canola:soybean

oil = 50:50) is −22 °C, all the exothermic and endothermic peaks depicted in Fig. 4 were due to the crystallization and melting of RBX. T_m decreased from 78.2 to 73.4 °C from pure bulk to 50% solution, and a further decrease in T_m was observed with a decreasing concentration of RBX. However, T_c did not differ from that of the pure bulk sample at RBX concentrations down to 40%, and gradually decreased with a further decrease in RBX concentration. Although the DSC patterns exhibited a high noise level because of the increase of salad oil, a sharp exothermic peak of crystallization was detected at 48.1 °C and an endothermic peak of melting was detected at 54.3 °C, even at an RBX concentration of 1%. However, such sharp crystallization and melting examined by DSC was not observed for CLX and CRX at a concentration of 1%. The molecular asymmetries between linear wax molecules compared to the oil molecules (triacylglycerols) which take a non-linear chair configuration in the solid state, are very different from each other. This molecular difference is responsible for rapid phase separation and crystallization of the wax solute from the oil solvent.

Figure 5 presents the average values of T_m and T_c of RBX in salad oil, liquid paraffin, and olive oil. It is clear that T_c did not decrease much from that of pure RBX with decreasing RBX concentration down to 40%, whereas T_c started to decrease below 30% in the three RBX–oil mixtures. In contrast, T_m gradually decreased with decreasing RBX concentration; the values of supercooling ΔT ($T_m - T_c$) decreased with decreasing RBX concentrations from 10 (pure) to 4 °C (20%), and reached as low as less than 2 °C at RBX concentrations below 20% for RBX–salad oil mixtures. The same tendency was observed in the mixtures of RBX–liquid paraffin and RBX–olive oil. This result indicates that the rate of crystallization of RBX in low concentration in salad oil is relatively high. Below the plotted T_c line, the RBX–liquid oil mixture is in a complete gel state, while above the T_m line it is in a complete sol state. Therefore, we conclude that the RBX–liquid oil mixtures tend to form a gel structure as soon as the temperature of the mixture decreases to the melting point below the RBX concentration of 20%. In particular, the gelation ability at room temperature (20 °C) was high even at very low concentrations of 1% (w/w) in salad oil and at the concentration of 0.5% (w/w) in olive oil.

Toro-Vazquez et al. [5] reported on the thermodynamic and kinetic properties of CLX–safflower oil mixtures, demonstrating that organogels formed above a CLX concentration of 1%. In this mixture, they measured

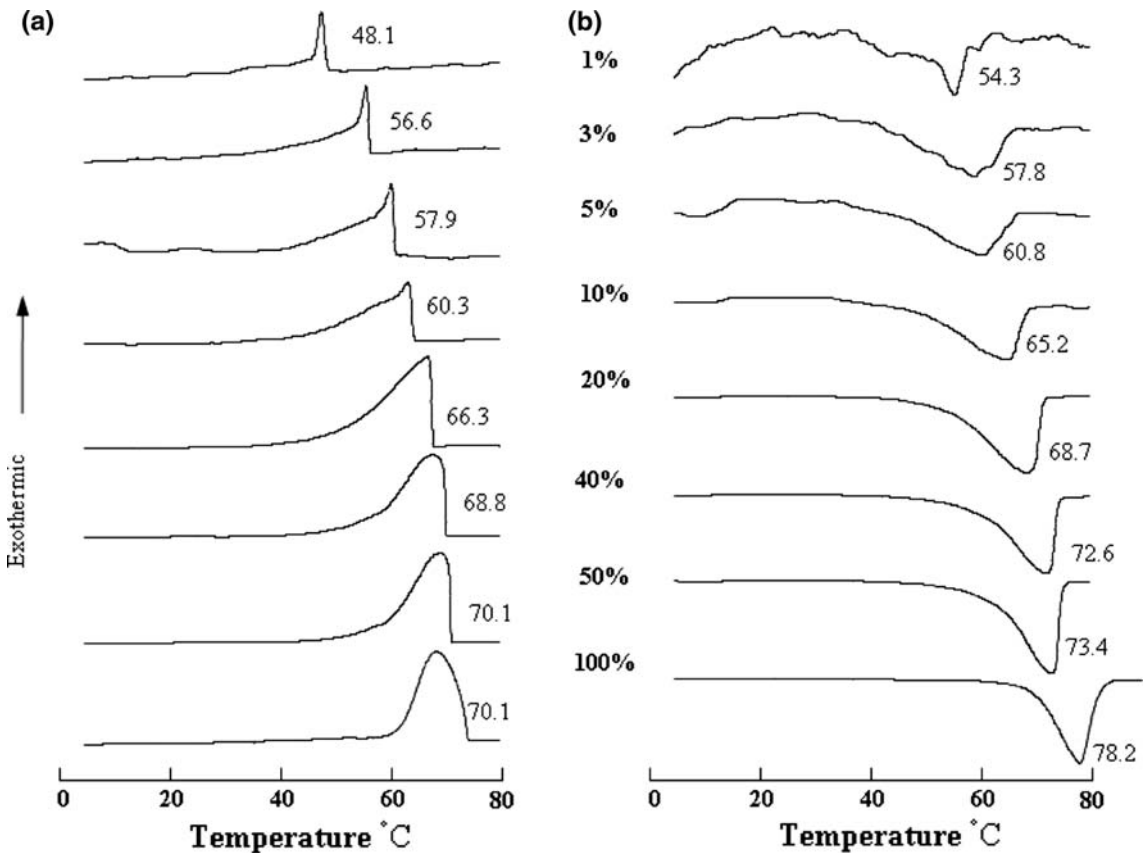

Fig. 4 DSC (**a**) cooling and (**b**) heating thermopeaks of rice bran wax (*RBX*) and salad oil mixtures at different concentrations of RBX

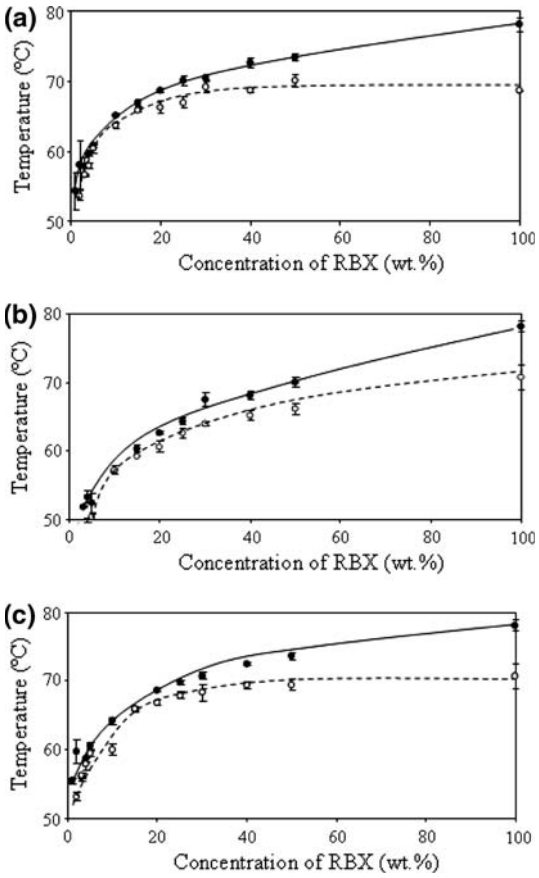

Fig. 5 Crystallization temperatures (*open circles*) and melting temperatures (*closed circles*) of rice bran wax (*RBX*) in (**a**) salad oil, (**b**) liquid paraffin and (**c**) olive oil

ΔT ($T_m - T_c$) of CLX in a range of CLX concentration of 0.5 to 6.0%, and found average ΔT values of 4.0 °C. By comparison, the ΔT values of RBX were small. Wright et al. [19, 20] presented phase diagrams constructed for ricinoelaidic acid (REA; 12-hydroxy, 9-*trans*-octadecenoic acid) as a gelator, and liquid canola oil and unrefined sesame oil. They observed that ΔT values largely depended on the concentration of REA and temperature. Comparison of the two gelating materials revealed that ΔT values of RBX–salad oil mixtures were less than 2° below 20 °C, indicating that organogels using RBX can be formed relatively easily.

To determine the kinetic properties of organogel formation, we measured the induction time of crystallization (τ_c) and gelation (τ_g) of RBX, CLX, and CRX in olive oil (Table 3). The induction time of crystallization (τ_c) was defined as the duration between the time when the temperature of the wax–olive oil mixture reached 20 °C and the time when crystallization was confirmed by optical microscopic observation. Similarly, the τ_g was defined as the time necessary for the oil to stop flowing after the sample was tilted to 45° at 20 °C. We found that τ_c and τ_g

Table 3 Induction time for crystallization (τ_c) and gelation (τ_g) of three plant waxes at different concentrations in olive oil at 20 °C

Concentration of wax (%)	τ_c (min:s)			τ_g (min:s)		
	RBX	CLX	CRX	RBX	CLX	CRX
0.2	6:1	*	4:5	•	•	•
0.5	2:4	*	2:1	10:5	•	•
1.0	1:4	7:4	1:3	7:2	•	•
2.0	1:0	4:4	1:0	6:2	13:5	•
4.0	0:3	3:1	0:4	4:4	9:2	13:5

*No crystals observed in 2 days

•No gelation observed in 2 days

were highly dependent on the wax concentration. However, τ_c of RBX and CRX was much shorter than that of CLX at any wax concentration. Although CRX formed crystals relatively faster than other waxes, it exhibited a weaker ability to form a gel, and the minimum wax concentration that could form a gel was 4.0% (w/w). The lowest concentration of CLX that exhibited crystallization was 1.0% (w/w), and the lowest concentration exhibiting gelation was 2.0% (w/w). RBX had high ability to form gel at a concentration as low as 0.5% (w/w), which is the lowest among the three waxes, since the minimum concentration of CLX that formed gels was 2.0% (w/w) and the minimum concentration of CRX that formed gels was 4.0% (w/w). Below these levels, no gelation was observed even after 2 days at 20 °C, even though crystallization was detectable in the wax–solvent mixtures. Although RBX formed crystals more slowly than CRX, it was much faster and more capable of gel formation. The gelation time of RBX in different oils decreased in the order of olive oil < salad oil < paraffin oil.

It has been reported that the nature of the organic solvent can also influence the aggregation of wax molecules [1]. Therefore, we measured τ_c and τ_g values in RBX–liquid paraffin and RBX–salad oil mixtures at 20 °C (Table 4). Crystallization and gelation occurred much faster in the RBX–salad oil mixture than in the RBX–liquid paraffin mixture at the same RBX concentration. No gelation was observed at a concentration of 0.5% (w/w) in paraffin and salad oil, although gelation occurred in olive oil at this level of RBX (Table 3). This result indicates that the properties of the solvent play an important role in plant wax–vegetable oil organogel formation.

As another kinetic property of gel formation, it is interesting to relate the occurrence of crystallization and gel formation in the two mixtures of RBX–olive oil and CLX–olive oil, in which the wax concentration was 1% (w/w). CRX was not examined, since its gel formation ability was quite low. Crystallization was observed by DSC, and gel formation was examined by viscosity measurement

Table 4 Induction time for crystallization (τ_c) and gelation (τ_g) of rice bran wax at different concentrations in liquid paraffin and salad oil at 20 °C

Concentration of wax (%)	Liquid paraffin		Salad oil	
	τ_c (min:s)	τ_g (min:s)	τ_c (min:s)	τ_g (min:s)
0.5	7:2	*	3:0	*
1.0	4:0	14:1	2:5	10:5
2.0	3:5	13:5	0:5	8:1
4.0	1:1	6:6	0:2	4:2
8.0	0:2	5:6	0:2	3:2

*No gelation

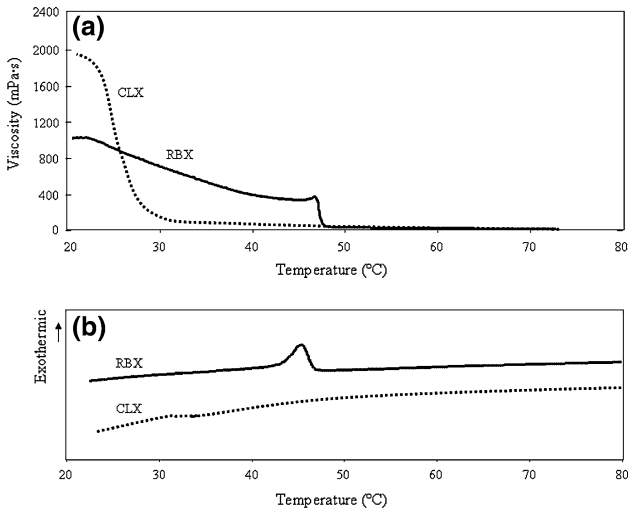

Fig. 6 Changes in (**a**) viscosity during cooling from 80 to 20 °C along with (**b**) DSC exothermic curves of different wax–olive oil mixtures

(Fig. 6). Upon cooling, the two wax gels revealed significant differences in viscosity–crystallization features. For the CLX–olive oil mixture, an exothermic DSC peak appeared at 33 °C, yet no increase in viscosity was observed until the temperature declined below 30 °C, whereas viscosity rose above 1600 mPa s below 25 °C. In contrast, the viscosity of the RBX–olive oil mixture started to increase and reached 400 mPa s soon after the DSC exothermic appeared at 46 °C, and its value gradually increased with decreasing temperature, reaching 1,100 mPa s at 20 °C. Therefore, it is evident that viscosity changes in the gels occurred parallel to the onset of crystallization for the RBX–olive oil mixture. This result is highly consistent with the results of visually examined kinetic properties of gel formation (Tables 3 and 4). For the CRX–olive oil 1% (w/w) mixture, no gelation was observed, although an increase in viscosity was observed at 20 °C (not shown). From these results, we conclude that the network formation of RBX crystals to reveal organogel properties occurred more rapidly coinciding with temperatures of crystallization than that of the mixtures of CLX and CRX in olive oil.

For the final result, we measured the hardness of the different levels of the three plant waxes and olive oil mixtures at 20 °C (Fig. 7). Since 1% (w/w) of RBX, CLX, and CRX and 3% (w/w) of CRX were in the sol state, no penetration experiments were conducted for those samples. The depth (mm) at which the penetration probe of the instrument penetrated in the gel was used to evaluate hardness, and large values of penetration depth meant softer gel structure. At a concentration level of 3%, the penetration depths of RBX–olive oil and CLX–olive oil mixtures were almost same. However, RBX exhibited greater hardness than CRX and CLX with increasing wax concentrations of 6 and 10%. In particular, the penetration depth of the RBX–olive oil mixture was half that of the CRX–olive oil mixture and 20% less than that of the CLX–olive oil mixture.

The effect of wax type on hardness and viscosity can be explained by crystal behavior, shape, size, and thermal kinetics. Fiber-like, smaller needle crystals lead to a

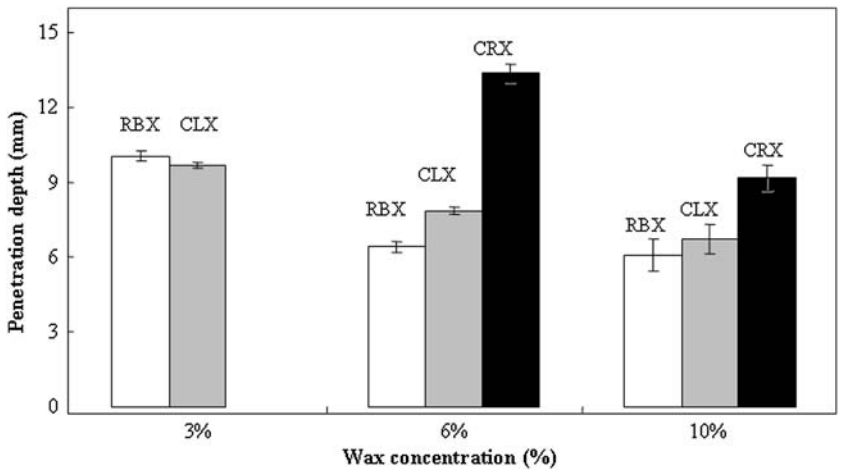

Fig. 7 Penetration depth of the organogels of three waxes in olive oil at different concentrations measured at 20 °C

stronger gel network formation, followed by high melting and crystallization points that cause high viscosity and hard gels. The comparatively longer fibrous crystals of RBX form a better gelator network that entraps the liquid oil, as evidenced in microscopy (Fig. 2) and gelation behavior (Tables 3 and 4).

The physical properties of organogels formed by RBX and liquid oils in comparison with other typical plant waxes of CLX and CRX can be summarized as follows. (a) The rate of formation of organogels was highest for RBX gels, as determined by visual observation and viscosity–temperature relationships. (b) The hardness assessed by the penetration depth measurement was highest for RBX gels. (c) Thermal stability expressed as the T_m of wax crystals in organogels was highest for RBX gels. These properties may be ascribed to the high crystallinity of RBX crystals having the greatest ΔH_m and ΔS_m, whose values are similar to those of the PPP β form. As PPP crystals are very tightly packed in the $T_{//}$subcell, it is reasonable to assume that the RBX crystals are also in tight packing in the $O_{\perp}$ subcell structures. The differences in the subcell structure may be responsible to the molecular differences between RBX and PPP structures. Furthermore, the crystal morphology of the needle shaped RBX crystals in organogels may indicate a better ability to entrap the liquid oils to form organogels.

References

1. Terech P, Weiss RG (1997) Low molecular mass gelators of organic liquids and the properties of their gels. Chem Rev 97:3133–3159
2. Abdallah DJ, Weiss RG (2000) Organogels and low molecular mass organic gelators. Adv Mater 12:1237–1247
3. Abdallah DJ, Sirchio SA, Weiss RG (2000) Hexatriacontane organogels. The first determination of the conformation and molecular packing of a low-molecular-mass organogelator in its gelled state. Langmuir 16:7558–7561
4. Pernetti M, van Malssen K, Kalnin D, Flöter E (2007) Structuring of edible oil with lecithin and sorbitan tri-stearate. Food Hydrocoll 21:855–861
5. Toro-Vazquez JF, Morales-Rueda JA, Dibildox-Alvarado E, Charó-Alonso M, Alonzo-Macias M, González-Chávez MM (2007) Thermal and textural properties of organogels developed by candelilla wax in safflower oil. J Am Oil Chem Soc 84:989–1000
6. Xiao Huang, Weiss RG (2007) Molecular organogels of the sodium salt of (R)-12-hydroxystearic acid and their templated syntheses of inorganic oxides. Tetrahedron 63:7375–7385
7. Pernetti M, van Malssen KF, Flöter E, Bot A (2007) Structuring of edible oils by alternatives to crystalline fat. Curr Opin Colloid Interface Sci 12:221–231
8. Bot A, Veldhuizen YSJ, den Adel R, Roijers EC (2009) Non-TAG structuring of edible oils and emulsions. Food Hydrocoll 23:1184–1189
9. Vintiloiu A, Leroux JC (2008) Organogels and their use in drug delivery—a review. J Control Release 125:179–192
10. Bot A, Agterof WGM (2006) Structuring of edible oils by mixtures of γ-oryzanol with β-sitosterol or related phytosterols. J Am Oil Chem Soc 83:513–521
11. Bot A, Adel R, Roigers EC (2008) Fibrils of γ-oryzanol + β-sitosterol in edible oil organogels. J Am Oil Chem Soc 85:1127–1134
12. Daniel J, Rajasekaran R (2003) Organogelation of plant oils and hydrocarbons by long-chain saturated FA, fatty alcohols, wax esters, and dicarboxylic acids. J Am Oil Chem Soc 80:417–421
13. Gandolfo FG, Bot A, Flöter E (2004) Structuring of edible oils by long-chain FA, fatty alcohols and their mixtures. J Am Oil Chem Soc 81:1–6
14. Schaink HM, van Malssen KF, Morgado-Alves S, Kalnin D, van der Linden (2007) Crystal network for edible oil organogels: possibilities and limitations of fatty acid and fatty alcohol systems. Food Res Intern 40:1185–1193
15. Tamura T, Ichikawa M (1997) Effect of lecithin on organogel formation of 12-hydroxystearic acid. J Am Oil Chem Soc 74:491–495
16. Rogers MA, Wright AJ, Marangoni AG (2008) Crystalline stability of self-assembled fibrillar networks of 12-hydroxystearic acid in edible oils. Food Res Intern 41:1026–1034
17. Rogers MA, Marangoni AG (2008) Non-isothermal nucleation and crystallization of 12-hydroxystearic acid in vegetable oils. Cryst Growth Des 8:4596–4601
18. Rogers MA, Wright AJ, Marangoni AG (2009) Nanostructuring fiber morphology and solvent inclusions in 12-hydroxystearic acid/canola oil organogels. Curr Opin Colloid Interface Sci 14:33–42
19. Wright AJ, Marangoni AG (2006) Formation, structure, and rheological properties of ricinoelaidic acid–vegetable oil organogels. J Am Oil Chem Soc 83:497–503
20. Wright AJ, Marangoni AG (2007) Time, temperature, and concentration dependance of ricinoelaidic acid–canola oil organogelation. J Am Oil Chem Soc 84:3–9
21. Murdan S, Gregoriadis G, Florence AT (1999) Novel sorbitan monostearate organogels. J Pharm Sci 88:608–614
22. Rogers MA (2009) Novel structuring strategies for unsaturated fats—meeting the zero-trans, zero-saturated fat challenge: a review. Food Res Intern 42:747–753
23. Small DM (ed) (1986) Handbook of lipid research 4. The physical chemistry of lipids from alkanes to phopholipids. Plenum, New York
24. Akoh CC, Min BD (eds) (2002) Food lipids chemistry, nutrition & biotechnology, 2nd edn. Marcel Dekker, New York
25. Martini S, Añón MC (2003) Crystallization of sunflower oil waxes. J Am Oil Chem Soc 80:525–532
26. Vali SR, Yi-Hsu Ju, Kaimal TNB, Yaw-Terang Chern (2005) A process for the preparation of food-grade rice bran wax and the determination of its composition. J Am Oil Chem Soc 82:57–64
27. Ghosh M, Bandyopadhyay S (2005) Studies on the crystal growth of rice bran wax in a hexane medium. J Am Oil Chem Soc 82:229–231
28. Morales-Rueda JA, Dibilox-Alvarado E, Charó-Alonso M, Weiss RG, Toro-Vazquez JF (2009) Thermo-mechanical properties of candelilla wax and dotriacontane organogels in safflower oil. Eur J Lipid Sci Technol 111:207–215
29. MD Idea Exporting Division. Uses and application rice bran wax, from octacosanol to phytosterol. http://www.mdidea.com/products/proper/proper059.html Accessed November 2008
30. Global Agritech Inc., (2009) Stabilization of long chain polyunsaturated oils. US Patent (PTC/US2008/071178)
31. Letcher CS (1983) Waxes. Kirk–Othmer encyclopedia on chemical technology, 3rd edn. vol 24, Wiley, New York, pp 466–81
32. Tulloch AP (1973) Comparison of some commercial waxes by gas liquid chromatography. J Am Oil Chem Soc 50:367–371

33. Tada A, Masuda A, Sugimoto N, Yamagata K, Yamazaki T, Tanamoto K (2007) Analysis of constituents of ester type gum bases used as natural food additives. Food Hyg 48:179–185
34. Cyber Lipid Center Waxes and other esters. http://www.cyberlipid.org/wax/wax0001.htm#2 Accessed July 2009
35. Sato K, Goto M, Yano J, Honda K, Kodali DR, Small DM (2001) Atomic resolution structure analysis of β' polymorph crystals of triacylglycerol: 1, 2-dipalmitoyl-3-myristoyl-sn-glycerol. J Lipid Res 42:338–345